IOP Conference Series: Earth and Environmental Science

PAPER • **OPEN ACCESS**

Development of small-scale downdraft gasifiers for biomass gasification

To cite this article: T M A Olayanju *et al* 2020 *IOP Conf. Ser.: Earth Environ. Sci.* **445** 012056

View the article online for updates and enhancements.

This content was downloaded from IP address 196.223.112.2 on 11/05/2020 at 11:43

Development of small-scale downdraft gasifiers for biomass gasification

T M A Olayanju[1,2], O.U Dairo[1], O Sobukola[1], O Odebiyi[1]and S O Dahunsi[2]
[1]Federal University of Agriculture, Abeokuta, Ogun State, Nigeria
[2]Agricultural Mechanization Group, Landmark University, Omu-Aran, Kwara State, Nigeria

Corresponding email: olayanju.adeniyi@lmu.edu.ng

Abstract. Biomass gasification mainly involves a process whereby agricultural residues or biomass are subjected to partial combustion for the biomass to undergo pyrolysis and reduction, thereby releasing its gaseous component such as hydrogen, carbon-dioxide and methane. Past studies have laid emphasis on the need to study the effect of moisture content and biomass types on the rate of gasification and gasifier efficiency. This study focused on the development of a downdraft gasifier for production of syngas using agricultural wastes as raw materials. The design of the Imbert type downdraft gasifier was based on specific gasification rate, called hearth load G_h, nozzle air blast velocities, throat inclination angle, air inlet diameter and size of reduction zone. The developed gasifier consisted of a reactor, cyclone and filtration unit of 0.006, 0.016, and 0.006 m^3 capacities respectively. The testing and evaluation of the designed gasifier showed adequate capacity for biomass treatment by pyrolysis. The fabricated gasifier also showed high efficiency in the pyrolysis of the selected biomasses and the product yields are appreciable. The development and use of such gasifier especially for the treatment of other agricultural wastes is hereby solicited.

1. Introduction

In recent years, biomass energy has gain a lot of attention due to its great potential of contributing to sustainable energy development [1-7]. The continuous recognition of biomass as one of the promising renewable sources of energy results from the gradual depletion of conventional fossil fuels [8,9]. Gasification, a thermo-chemical partial oxidation process, has superb capacity for biomass power recovery, as it is able to convert biomass into syngas commonly known as combustible gases, which can be further converted to electricity and biochar that has a large carbon sequestration capability [10]. Also, biomass gasification is one of the key technologies to convert waste biomass or carbonaceous materials to syngas efficiently and economically. Syngas is the source for high-value chemicals (such as methanol, DME) [11] and liquid carbohydrates [1]. By so doing, the issue of environmental pollution which is ubiquitous especially in the Sub-Saharan Africa, resulting from waste can be combated [12-15]. According to You et al. [16], balancing syngas and biochar production is an economically and environmentally friendly (greenhouse gas mitigation) gasification system can be developed.

Gasifier (a gasification device) design is a crucial step to optimize the economics and green potential of a gasification system to reach cleaner energy production. Gasifiers are the main devices used for gasification; they perform the conversion process of biomass to syngas, consisting mainly of CO, CO_2,

Content from this work may be used under the terms of the Creative Commons Attribution 3.0 licence. Any further distribution of this work must maintain attribution to the author(s) and the title of the work, journal citation and DOI.
Published under licence by IOP Publishing Ltd

H_2, N_2, ashes, tar and small particulates [17]. Past researches have recorded three principal types of gasifiers, which includes fluidized bed gasifiers [18], entrained flow gasifiers [19] and fixed bed gasifiers [20]. Among the various technologies that can be used for biomass combustion, fluidized beds are gradually emerging as the best due to their flexibility with respect to the type of fuel and high efficiency. One major problem of fluidized beds is defluidization due to bed agglomeration; high amounts of oxygen bypass the reactor bed due to the low level of oxygen dissemination from the gas bubbles, which reduces the efficiency of the gasifier. However, successful solution has been reported for other biomass feedstock [21]. In an entrained flow gasifiers, syngas with a lower tar content are been produced and about 20% more oxygen is required [22]. The oldest and common reactors employed to synthesize syngas are the fixed bed gasifiers. Higher than 10MW (that is, large scale) fixed bed gasifiers are losing the interests of industrial units due to scale-up issues [23], however, small scale fixed bed gasifiers with high thermal efficiency are in use for decentralized energy generation and for thermal applications in many industries [24]. Fixed bed gasifiers can be further divided into updraft [25] or downdraft [26] based on the gas flow direction. Due to its simplicity and tractability, the updraft gasifier is one of the oldest types of gasifier. It is termed "updraft" because the biomass is fed from the top of the gasifier, while air is supplied at the bottom of the gasifier. On the other hand, air move in the downward direction in the lower section of the downdraft gasifier unit.

In downdraft bed gasifiers, tar content is much lower compared to that in an updraft gasifier, but the syngas has less calorific value [22]. Downdraft gasifier is more suitable for small-scale applications [27]. Downdraft gasifiers are the most widely deployed gasification technique in small-scale applications and it was reported that around 75% of gasifier manufacturers in Europe produce downdraft gasifiers [28]. A review of 50 gasifier manufacturers in Europe, United State and Canada showed that 75% of the designs were downdraft fixed beds while fluidized beds, updraft fixed beds and the other designs were 20%, 2.5%, 2.5%, respectively [29]. As far as Nigeria is concerned and because of its vast agro-forestry base, fuels of bio-origin can be considered to be ideal alternative renewable fuels to run the internal combustion engines. The bio-origin fuels could be modified to bring their properties comparable to fossil fuels. A downdraft gasifier usually consists of four sequential zones, i.e. drying zone, pyrolysis zone, combustion zone, and reduction zone, respectively, among which the reduction zone is responsible for syngas production [22].

2. Materials and Methods

2.1. Design Concept

The concept of this design was fashioned after Imbert type of gasifier design mainly for downdraft gasifiers because of its wide acceptability and use among design engineers. The design of an Imbert type downdraft gasifier is based on specific gasification rate, called hearth load G_h, nozzle air blast velocities, throat inclination angle, air inlet diameter and size of reduction zone. The developed gasifier consisted of a reactor (for gasification), cyclone (for cooling) and filtration (for cleaning) unit of 0.006, 0.016, and 0.006 m^3 capacities respectively. This is defined as the ratio of Volume of gas to cross-sectional Area of the throat and it is given by equation 1.

$$GH = \frac{V}{A} \quad (1)$$

Where:

V= Volume of producer gas,

A = Cross-sectional area of the throat

The gas volume is calculated at normal pressure and temperature. Its values range from 0.1 to 0.9 m^3/ cm^2. Figure 1b depicts a simple system of Imbert type of gasifier.

2.2. The Gasifier Components

The conceptual gasifier design is made of three main parts which are: reactor chamber, cooling unit and the Filtering unit.

2.3. Reactor Section

The reactor chamber is the main unit where gasification process occurs. This is a chamber which comprises of inner and outer cylinders. The inner cylinder is usually made of stainless steel so as to withstand the high temperature it will be subjected to. The outer cylinder can be made of mild steel and it serves as housing for the inner chamber to minimize the heat loss or gain into the surroundings. The biomass is been fed into the reactor chamber where processes like drying, pyrolysis, oxidation and reduction take place before the eventual liberation of the syngas. The various design parameters of the reactor chamber are the diameter of the reactor, height of the reactor, diameter of hearth and throat, air velocity, diameter of gas outlet, length of the pipe for the gas outlet, surface Area of air inlet and throat angle.

2.4. Cooling Section

This unit consists of a cyclone which cools the temperature of the gas as it enters from the reactor chamber. This is the section where the various impurities like tar will be collected and separated from the syngas. It is usually in form of cyclone to allow a free fall of the impurities into the tar collection chamber at the conical base. Also, a cooling fan was attached to the filtering section. The various design parameters for the cyclone unit are; the height of the cyclone, diameter of the cyclone, taper angle at the bottom, diameter of the base, gas inlet diameter and gas outlet diameter

2.5. Filtering Unit

This section is made of cylinder chamber filled with the filtering medium in order to remove other impurities inform of particles from the gases before final use. The various parameters of the cyclone are the height of the filter, diameter of the filter, gas inlet diameter and gas outlet diameter. The composition of various types of gasifiers available during the World War II indicated that the maximum specific gasification rate (or hearth load) is of the order 0.09, 0.03 and 0.9 Nm^3/hcm^2 for no throat, single throat and double throat gasifier respectively. This information is useful in order to have an idea of the range of gasification rate to use in this design.

2.6. Design Criteria for Gasifier Reactor

The following recommendations were given by FAO [30] in 1986 as the guidelines to the design of down-draft gasifier as shown in table 1.

i. Nozzle air-blast velocities should be of the order of 22- 33m/s
ii. Throat inclination angle should be about 45^o - 60^o.
iii. Hearth diameter at the air inlet should be 0.01m and 0.02m larger than the smallest cross-section (throat) in the case of single and double –throat design respectively.
iv. Reduction zone height should be more than 0.02 m
v. Air inlet nozzle plane should be located more than .0.01m above the throat section.

Table 1. Design Parameters and Values for Gasifier Reactor

Parameters	**Value (m)**
Height of reactor (H)	0.700

Outer Diameter of reactor (Df)	0.210
Diameter of inner cylinder (Dn)	0.150
Throat Diameter (dt)	0.060
Height of nozzle plane (h)	0.052
Diameter of ignition port (dm)	0.136
Diameter of the outlet pipe	0.05
Length of outlet pipe	0.40

2.7. Gasifier Design Calculations

In order to have a proper design, the idea of the capacity of the engine the gasifier will be able to carry is needed, and in this case, 5.0 KVA engine was considered. A typical 5.0 KVA engine have the following engine parameters which are useful for the design of the gasifier reactor.

Rated Output = 5.0 KW (13 HP)

- Piston Diameter = 88.00 mm
- Stroke length = 64.0 mm
- Number of cylinder = 1 (4 stroke cycle)
- Engine RPM = 3,600
- Operation hours = 10 hours
- Volumetric Efficiency = 85 %

2.8. Reactor Design Steps

The first step is to find out the required gas production rate.

Since Engine Swept Volume (V_s) equals,

$$V_s = ½ * RPM * N * A * S \quad (2)$$

Where N = number of cylinder

A = Area (m^2)

S = Stroke (m)

Substituting the values given in the 5KVA engine parameters into equation (2) as stated above:

$$Vs = \frac{1}{2} * 3600 * 1 * 0.064 * \pi d^2$$

Vs = 42.05 m^3/h

Using stoichiometric air-fuel (gas) ratio 1.1: 1.0, for the intake volume of gas (V_g), the air-fuel intake will be 2.1.

Equation 9 stated below shows the relationship between the Swept volume, Volume of gas and volumetric efficiency of the engine.

$$Vg = f * \frac{Vs}{2.1} \quad (3)$$

Where V_s= Swept Volume of the engine = 42.05 m^3/h

V_g= Volume of the gas (m^3/h)

f = volumetric efficiency = 85 % = 0.85

Substituting into the values into equation (3) above, the value of V_g is:

Vg = 17.0 m^3/h

For maximum hearth load G_H of 0.9 m^3/cm^2, the throat Area A_t, can be calculated from equation 4

$$A_t = \frac{Vg}{Gh\max} \quad (4)$$

Where A_t = Area of the reactor throat (m^2)

V_g= Volume of the gas (m^3/h) = 17.0 m^3/h

G_H= Gasification rate = 0.9 m^3/cm^2

By substituting the values above into equation (3)

A_t = 18.90 cm^2 = 0.00189 m^2

Choosing Hearth Load G_h = 0.7 Nm^3/hcm^2 (As recommended by Imbert)

Substituting into equation (3) above

A_t = 24.29 cm^2 = 0.0024 m^2

For this design, hearth load of 0.7 will be used since is closer to the maximum hearth load (0.9) and it was also recommended by Imbert in his design. Thus, the throat diameter d_t for the circular cross-sectional can be obtained from equation (5).

$$A = \frac{\pi d^2}{4} \quad (5)$$

Where D = d_t is the diameter of the throat

Where A_t = 0.0024 m^2

d_t = 0.0556 m

Therefore, the diameter of the throat will be taken approximately 0.056m.

Using the graph of h/ d_t as against d_t as prepared by Swedish Academy of Engineering Sciences. As shown in figure 1d below:

At dt = 6cm = 60mm, on the positive x-axis, on the positive y-axis

Where h = height of nozzle above the throat.

d_t = diameter of the throat

$$\frac{h}{dt} = 1.3 \tag{6}$$

h = 78 mm = 0.078m

The diameter of firebox d_f and the diameter of nozzle top ring d_n can be determined using the graph of (against d_t). Also, graph of (against d_t), as obtained from FAO [30] in 1986 shown in Figure 1b.

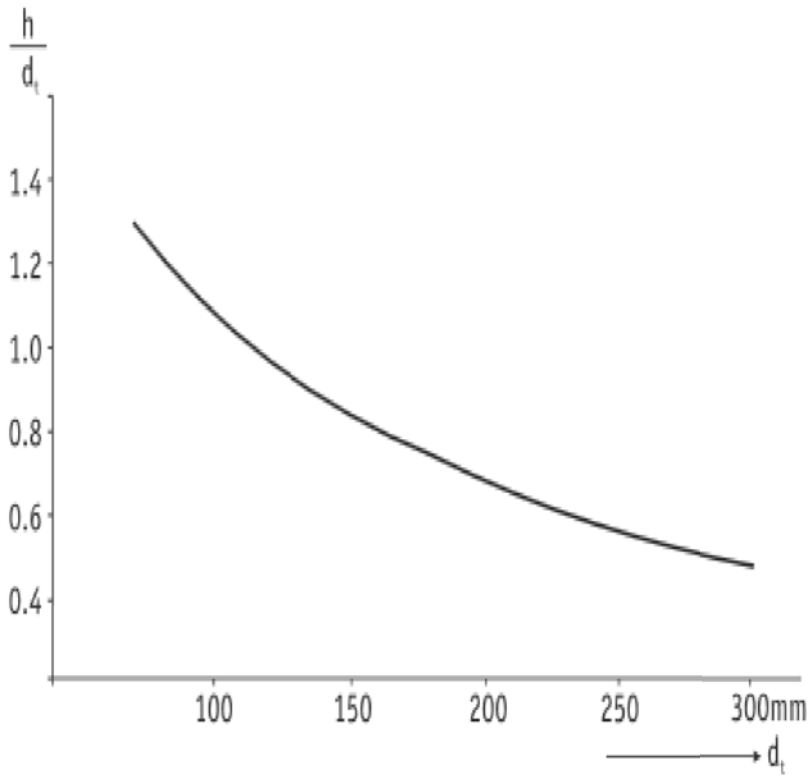

Figure 1a. Height of nozzle plane above throat for various diameters, FAO (1986)

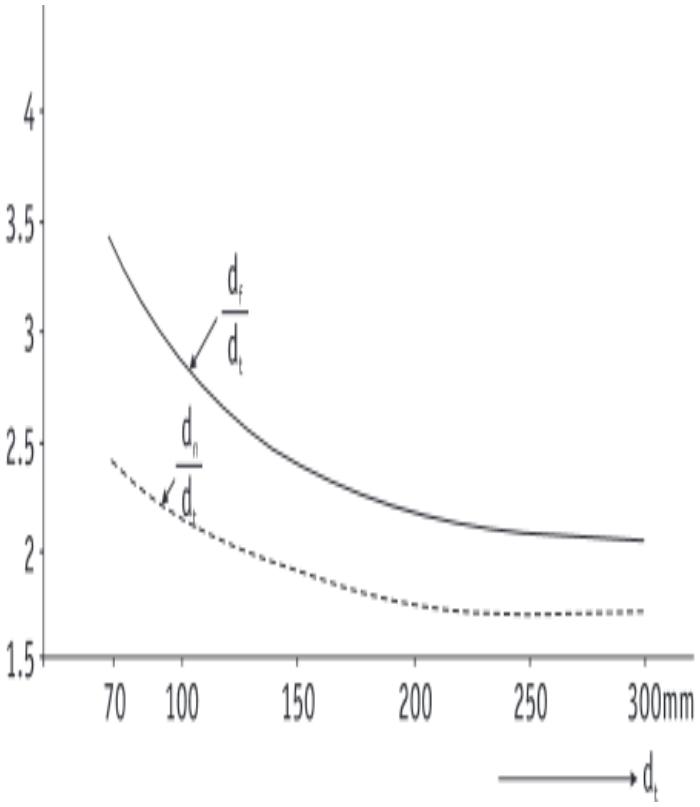

Figure 1b. Nozzle ring diameter as a function of throat diameter Reproduced with permission from FAO

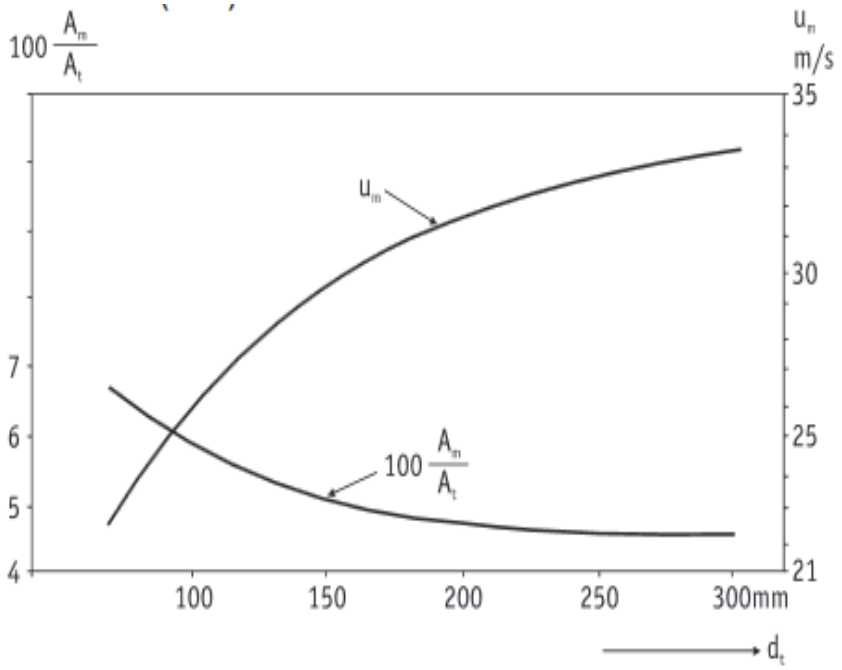

Figure 1c. Nozzle area for various gases of gasifier throat and blast velocities

From Figure 1b, the values are 3.5 and 2.5 respectively.

At d_t = 60mm = 0.06m

$$\text{And } \frac{dn}{dt} = 3.5 \tag{7}$$

Where d_n = diameter of the inner chamber, d_f = diameter of the outer chamber

Substituting the value of the throat diameter then, at d_t = 0.06m:

d_f = 0.21m

d_n = 0.15 m

Assuming that a unit of nozzles is to be used for supporting the required amount of air for gasification such that the ratio of 100 ($\frac{Am}{At}$) against d_t as shown in the gasifier graph (Figure 6) prepared by Swedish Academy of Engineering Sciences and reproduced by FAO [31] in 1960 at d_t = 6.0 cm.

Where A_m = Area of ignition port.

dt = 60mm = 6.0cm,

A_t = Area of the throat

$$100 \left(\frac{Am}{At}\right) = 6.0 \tag{8}$$

By substituting the value of A_t= 24.29cm^2 into equation (8)

$A_m = 6.0 \times 24.29$

$A_m = 145.74\ cm^2$

Diameter of the ignition port Air-inlet

$d_m = 13.6\ cm = 0.136\ m$

Also, the equivalent Air- blast velocity can be determined from Figure 1c as Um = 23 m/s.

Height of outer cylinder can be determined by adding allowance to the height of the inner cylinder. Since the height of the inner cylinder is 0.50m, then 0.10m was added at the bottom and top of the inner cylinder and the height of the outer cylinder will be 0.70m.

2.9. Pipe Fittings

Diameter of the pipe in the design will be taken as 2 inches = 5cm. The reason for chosen 5cm diameter pipe is to give room for the gas to move freely and also give room for the gas to cool down and release some of its heat to the pipe.

2.10. Cyclone Design

As shown in table 2, the cyclone design is to produce some level of gas cooling and cleaning. As the gas leaves the reactor, the temperature is appreciably high and its temperature reduces as it travels through the pipe into the cyclone chamber. The temperature further reduces inside the chamber as the gas molecules spins. The tar spins and fall under gravity as both the gas and particles spin in the cyclone chamber.

Table 2. The summary of parameter values for the cyclone design

Parameter	**Value**
Length of cyclone body (m)	0.50
Length of cone (m)	0.20
Diameter of cyclone (m)	0.01
Width of inlet duct (m)	0.05
Diameter of cyclone base	0.04
Number of spins (Ne) s	12
Gas residence time (T) s	0.164
Terminal Velocity (Vt) m/s	0.305
Tapered angle cyclone (degrees)	8^o

2.11. Design Parameters

A typical cyclone is shown in the figure 1d with all the parameters as shown. The design parameters to be considered in the cyclone are:

The general guidelines for the design of cyclone as related to the various geometry dimensions are as specified by Gasifier Design Handbook [30] are as listed below:

i. $H < S$
ii. $W < (D - De)/2$
iii. $Lb + Lc > 3D$
iv. $7° \leq \alpha < 8°$

v. $0.4 \leq \leq 0.5$
vi. $= 8$
vii. $= 1$

The values for the cyclone parameters are as stated below:
Length of cyclone body L_b = 0.50m (taken from the height of the inner cylinder in the reactor design).
Length of cyclone base Lc= 0.20 m (taken from the reactor design, base of the reactor)
Width of inlet duct w = 0.05 m
Cyclone Diameter D = 0.10 m
Height of inlet duct H = 0.0508 m
Diameter of the cyclone base = 0.0508m
Taper angle at the bottom = α

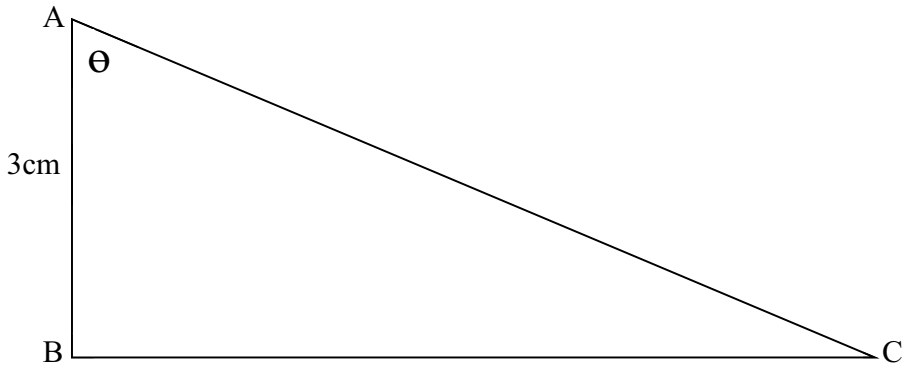

Figure 1d. Triangular representation of the design parameters

The triangle ABC as shown above depicts the base of the reactor and the falling angle for the biomass needs to be calculated. The reactor needs a conical base in order to allow the burnt biomass to find its way down to the collecting chamber at the base of the reactor as ash. From Triangle **ABC**, we can determine the angle of fall of the reactor base:

Since opposite BC = 20 cm

Adjacent **AB** = 3 cm

Then angle **BAC** can be calculated as:

T**an Θ** = 20/3

Tan Θ = 6.67

Θ = arc Tan 6.67

Θ = 81.47^0, so α = 8^0

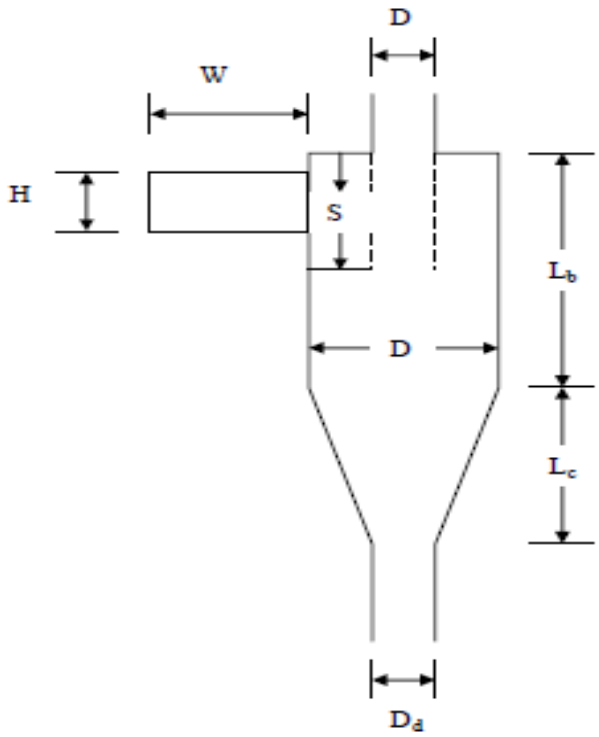

Figure 1e. A typical cyclone for gas cooling and cleaning with the following;

i. Hc = Height of cyclone
ii. Dc = Diameter of cyclone
iii. α = Taper angle at the bottom
iv. D_{cb}= Diameter of cyclone base
v. G_{id} = Gas inlet diameter
vi. G_{ii} = Gas outlet diameter

2.12. The Collection Efficiency

Gas spins through a number of revolutions **Ne,** given by equation 14 below (Cooper and Alley 1986)

$$\text{Ne} = \frac{1}{H}\left(Lb + \frac{Lc}{2}\right) \tag{9}$$

Where L_b= Length of cyclone body (m)

Lc = Length of cyclone base (m)

H = Height of inlet duct (m)

Substituting values of L_b, Lc and H

Ne = 12 turns.

Consequently, by design the gas enters the cyclone and spins 12 times before reaching the base of the cyclone. The gas molecules falls freely under the influence of gravity, the thicker impurities which happen to be the impurities or the char are collected at the base of the cyclone.

2.13. Gas Residence Time

Gas residence time is the average amount of time that a particle spends in a particular system in this case the cyclone. It can be a probability distribution function that describes the amount of time a fluid element could spend inside a chemical reactor.

The residence Time is given by equation 10 stated below;

$$T = \frac{\Pi DNe}{Vi} \tag{10}$$

Where

T = the residence time

D = the cyclone diameter = 10cm

Ne = the number of spins = 12

Vi = inlet velocity of the gas = 23 m/s

Substituting the values into the equation 9, then the residence time T

$$T = \frac{3.142 * 0.1 * 12}{23}$$

T = 0.164s

2.14. Terminal Velocity

The terminal velocity Vt of the particles in a radical direction that will just allow a particle initially at distance W away from the wall to the collected air time is given by equation 11:

$$Vt = \frac{W}{Dt} \tag{11}$$

Where, V_t is the terminal velocity i.e. the velocity at which drag force equals the resisting force, W is the width of the inlet duct

Substituting the values into equation 16, then Vt = 0.305 m/s

2.15. Filtering Section

The filtering section shown in Figure 1e is to remove the impurities that come with the syn-gas as its leaves the cyclone section. The height of the filtering section and the diameter can be chosen conveniently considering the size of the reactor. At least the dimension of the filtering section to be chosen must be relatively close to that of reactor. So, that account for the values chosen and stated below:

i. Height of filtering cylinder = 0.50 m
ii. Diameter of filter = 0.20 m

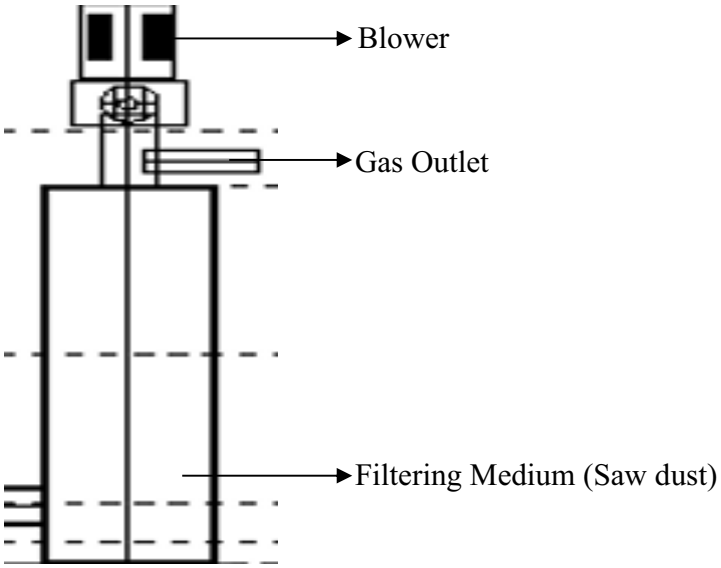

Figure 1f. Cross -section of the Filtering Unit

2.16. Materials Selection

The gasifier reactor section will be subjected to great temperature, so a stainless steel is needed in order to withstand the temperature of the gasification reaction. Also, mild steel is needed for the outer cylinder. The various materials selected for the construction of the gasifiers various components are as listed in Table 3. The various instrument needed for taken measurement during and after gasifier construction are as listed in table 4.

Table 3. Material selection for reactor, cyclone and filtering section

S/N	Component	Material selected
1	Gasifier Reactor (Inner Cylinder)	Stainless steel
2	Gasifier Reactor (Outer Cylinder)	Mild steel
3	Gas Outlet Pipe	Galvanized pipe
4	Cyclone Section	Mild Steel
5	Cyclone gas inlet and outlet	galvanized pipe
6	Filtering Section	Mild Steel
7	Gasifier Stand	Angle Iron
8	Gas Passage	Galvanized pipe

Table 4. Measuring instrument and their area of application

S/N	Instrument	Function
1	Thermocouple	Measures oxidation temperature
2	Thermometer	Measures Ambient temperature
3	Weighing Scale	To measure the amount of biomass and ash content
4	Drying Oven	To determine the moisture content of the biomass
5	Stop Watch	Measures time taken for complete gasification

2.17. Fabrication and Assembly

Fabrication of the various sections and components was done at the Central Workshop of the College of Engineering, Federal University of Agriculture, Abeokuta (FUNAAB) and those fabricated components were assembled together (Figures 2a and b).

Figure 2a. Cleaning and Filtering Unit assembled together (Before painting)

2.18. Feedstock

The feedstock used in this study are Saw dust, Wood chips, and Bean chaff. They were selected and experimented on the basis of availability and suitability for renewable energy generation since they are all lignocelluloses [32].

2.19. Biomass preparation

Each biomass was sundried till constant weight was achieved. Wood chips and Bean chaff were then crushed in a hammer mill so that all three biomasses achieved mean diameter of 10 to 30 μm. Mean bulk densities (ρb) of all biomasses ranged between 573 and 582 kg m^{-3} while their unit densities (ρu) ranged between 1331-1420 kg m^{-3} (EN 15103 - 2009). The lower heating value (LHV) for the biomasses ranged between 11.84 and 12.21 MJ kg^{-1} for the raw sample while it was between 12.99 and 13.31 MJ kg^{-1} for the dry sample respectively. Also, the higher heating values (HHV) ranged between 14.42 and 14.53 MJ kg^{-1} for the raw biomasses while it was between 14.94 and 15.31 MJ kg^{-1} for dry biomasses (ASTM D 5865-13). In all, the first deformation, softening and hemisphere temperatures (ASTM D 1857/D1857) were 1025, 1125, and 1317 °C, respectively.

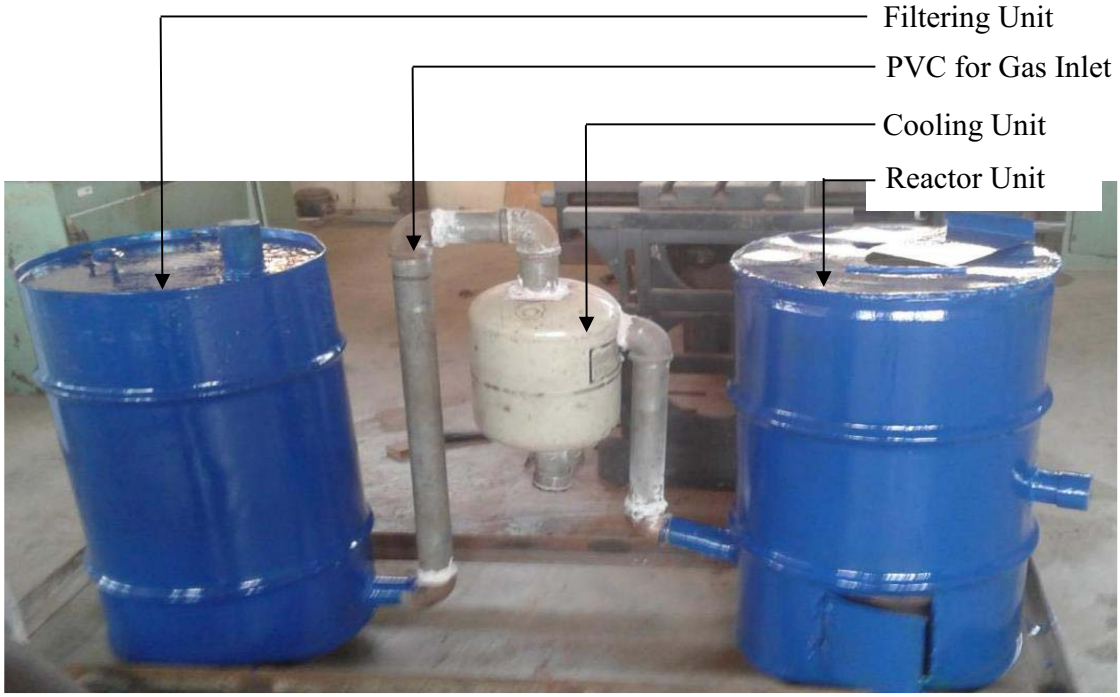

Figure 2b. Complete assembly of the gasifier

2.20. Biomass proximate analyses

As shown in tables 5a, the concentrations of total and volatile solids and ash were determined using the standard method for analysis of water and wastewaters [33]. The same method was used for the determination of Chemical Oxygen Demand (COD) in all the samples. The concentrations of parameters including carbon, phosphorus, phosphates, sulphates, potassium, sodium, magnesium, calcium, nitrates, ammonium, iron, copper, zinc, aluminium and manganese were determined with the aid of an inductively coupled plasma mass spectrometry. For pH measurement, 1 g of ground sample of each biomass was dissolved in 20 cm^3 of water and then incubated at 25 °C for 30 min after which the supernatant was used for the measurement with the aid of the HI 2211 pH/ORP Meter electrode (Hanna Instruments, Germany). For total organic carbon (TOC) determination, a SSM-5000A TOC analyzer (Shimadzu, Japan) was used while the Kjeldahl method was employed in analyzing the content of total Kjeldahl nitrogen. Volatile fatty acids (VFAs) concentrations were determined using standard method as described by Monlau et al. [34].

Table 5a. Proximate composition of used lignocelluloses

Parameter	**Saw dust**	**Wood chips**	**Bean chaff**
Ash Content (%)	3.6±0.01	4.2±0.01	3.6±0.03
Moisture Content (%)	45.7±1.01	52.2±1.01	58.3±3.05
Total Carbon (g/kg TS)	241.5±4.01	246.2±5.02	319.5±4.01
Total Nitrogen (g/kg TS)	9.3±0.02	10.2±0.02	45.4±0.05
Uronic acids (% VS)	1.0±0.01	1.2±1.10	1.47±0.02
Soluble sugars (% VS)	3.6±0.01	4.1±1.02	1.6±0.01
Phenols (mg L^{-1})	-	-	-

Total Phosphorus (g/kg TS)	3.4±0.01	2.1±0.11	4.3±0.01
Potassium (g/kg TS)	4.6±0.01	5.2±0.01	7.1±0.01
Phosphate (g/g TS)	1.2±0.01	2.01±0.01	1.9±0.01
Sulphate (g/kg TS)	40.4±1.00	46.2±2.00	36.5±0.01
Calcium (g/kg TS)	167.1±2.02	181.4±0.42	81.1±4.01
Magnesium (g/kg TS)	45.3±1.02	50.6±0.02	65.3±2.01
Iron (g/kg TS)	0.2±0.01	0.2±0.01	0.6±0.01
Zinc (g/kg TS)	1.2±0.01	1.1±0.01	2.1±0.01
Aluminium (g/kg TS)	26.7±0.01	25.3±0.02	35.4±1.01
Copper (g/kg TS)	1.2±0.01	1.3±0.02	1.6±0.01

N = 80

2.21. Structural characterization of biomass

As shown in table 5b, the structural composition (lignin, cellulose, hemicellulose and arabinan) of all the biomasses was determined using a standard method [35]. In order to determine the extractable materials in the biomasses; a Soxhlet extractor was employed for 6 h while samples of each biomass was burnt in a muffle furnace for the determination of fixed solids [35]. For the structural compositions, 0.3 g dried sample of each biomass was treated with 3 mL of 72% sulfuric acid ($v.v^{-1}$) in a thermostatic bath at 30 °C for 1 h while the resulting filtrate was used for carbohydrate determination [36]. The carbohydrates were analyzed using a liquid chromatography-mass spectrometer (LC–MS) (SHIMADZU, Japan) operated with AMINEX® BIORAD HPX87H column in refractive index detector (DIR-10A). The mobile phase in this analysis was 0.005 $mol.L^{-1}$ sulfuric acid in an isocratic mode, at 45 °C, with an injection volume of 20 µL and flow of 0.6 $mL.min^{-1}$. Calibration curves were used to determine the final concentrations of the compounds using specific LC–MS standards [37]. All samples were analyzed in triplicates.

Table 5b. Structural characterization of biomasses

Parameter	**Saw dust**	**Wood chips**	**Bean chaff**
pH	7.66±0.01	7.69±0.10	7.63±0.10
Total solids (% $m.m^{-1}$)	83.5±2.01	87.3±4.01	64.2±2.12
Volatile solids (% $m.m^{-1}$)	51.1±3.01	53.5±1.01	57.6±2.01
Total Lignin (% $m.m^{-1}$)	49.5±3.01	45.3±2.01	29.4±0.30
Cellulose (% $m.m^{-1}$)	33.3±2.01	36.5±1.50	17.4±0.01
Hemicellulose (% $m.m^{-1}$)	11.8±0.11	10.2±2.01	5.3±0.01
Arabinan (% $m.m^{-1}$)	2.4±0.01	3.1±0.05	0.8±0.01
Protein (% $m.m^{-1}$)	2.2±0.01	3.0±1.01	14.6±0.01
Fixed solids (% $m.m^{-1}$)	2.0±0.01	2.4±0.03	1.1±0.05
Extractives (% $m.m^{-1}$)	ND	ND	ND

Values shown in table are means of triplicate analyses with respective standard errors; ND = Not determined

2.22. Biomass gasification

The designed gasifier was employed in the pyrolysis of the three different biomasses using air as the gasification agent. The gasifier was designed to allow working with two different airflow inlets i.e. from both top and the tuyeres. Analyses of the biogas major components (CH_4, CO_2, H_2S and N_2) were carried out using infrared and electrochemical sensors (BIOGASS5000, USA).

3. Results and Discussion

The test results showed that the three biomasses (Saw dust, wood chips, Bean chaff) at 10% moisture level produced the least ash content. The ash contents at 10, 20 and 30% moisture contents for wood chips, sawdust and bean chaff were 0.210, 0.457, 0.750 kg; 0.202, 0.290, 0.651 kg and 0.295, 0.228, 0.394 kg respectively. The gas samples were taken at 10% moisture for analysis because it produced the lowest ash content. Gas produced at 10% moisture content showed that methane (CH_4), Carbon dioxide (CO_2),

Hydrogen sulfide (H_2S) and Nitrogen (N_2) contents for wood chips; sawdust and bean chaff were 60.85, 27.50, 0.44, 10.2%; 62.33, 23.77, 0.87, 8.5% and 63.94, 18.91, 0.58, 10.6% respectively. The values of CO was insignificant. The moisture content of the biomasses significantly ($p < 0.05$) affected the values of ash content, gasification time and temperature but the effects of biomass types were not significant. Ash content and gasification time increased with increase in moisture level with the least value of 0.210 kg and 61 minutes at 10% moisture content respectively. The gasification temperature decreased as moisture level increased and vice versa. Increase in moisture level increased the ash content and gasification time. The gasification temperature also increased as the gasification time reduced. Gasifier efficiency was also affected by moisture content and biomass types. The best gasifier efficiency was observed at 10% moisture content level with 60, 57 and 75% for sawdust, woodchips and bean chaff respectively. These results are in agreement with previous findings [38-48]. The temperature of the cooling unit after filter was measured to be 40^0C with the aid of hand-held digital thermometer.

4. Conclusion

This study focused on the design of an imbert type of gasifier design (Figure 2b). Gas storage facility can also be considered in the other research work. The fabricated gasifier also showed high efficiency in the pyrolysis of the selected biomasses and the product yields are appreciable.

Conflict of Interest
Authors declare that there are no conflicts of interest whatsoever. All authors agrees to this submission

Acknowledgements
The authors appreciates the efforts of our laboratory staff who contributed to the success of this research

Notation
APHA = American Public Health Association
COD = Chemical Oxygen Demand
FAO = Food and Agricultural Organization
KW = Kilowatt
KVA = Kilo Volt-ampere
LC-MS = Liquid Chromatography- Mass Spectrometer
RPM = Rotation per Minute
TOC = Total Organic Carbon
VFAs = Volatile Fatty Acids

References

[1] Jiang Y and Bhattacharyya D 2016 Techno-economic analysis of a novel indirect Coal–biomass to liquids plant integrated with a combined cycle plant and CO_2 capture and storage. *Ind. Eng. Chem. Res.* **55** 1677–89.
[2] Al-Rubaye H, Karambelkar S, Shivashankaraiah M M and Smith J D 2017 Process simulation of two-stage anaerobic digestion for methane productio. *Biofuels* **1** 181-91
[3] Dahunsi S O, Olayanju A, and Adesulu-Dahunsi A T 2019 Data on Optimization of bioconversion of fruit rind of *Telfairia occidentalis* (Fluted Pumpkin) and Poultry manure for biogas generation. *Chemical Data Collect* **20** 100192
[4] Dahunsi S O, Adesulu-Dahunsi A T and Izebere J O 2019 Cleaner energy through liquefaction of Cocoa (*Theobroma cacao*) pod husk: Pretreatment and process optimization. *J. Clean. Prod.* **226** 578-88
[5] Dahunsi S O, Adesulu-Dahunsi A T, Osueke C O, Lawal A I, Olayanju T M A, Ojediran J O and, Izebere J O 2019 Biogas generation from Sorghum bicolor stalk: Effect of pretreatment methods and economic feasibility. *Energy Reports* **5** 584-593.
[6] Dahunsi S O, Osueke C O, Olayanju T M A and Lawal A I 2019. Co-digestion of *Theobroma cacao* (Cocoa) pod husk and poultry manure for energy generation: Effects of pretreatment methods. *Bioresour. Technol.* **283** 229–41.

[7] Dahunsi S O 2019. Mechanical pretreatment of lignocelluloses for enhanced biogas production: Methane yield prediction from biomass structural components. *Bioresour. Technol.* **280** 18-26.
[8] Ohimain E I and Izah S.C 2017. A review of biogas production from palm oil mill effluents using different configurations of bioreactors. *Renew. Sustain. Energy Rev.* **70** 242–53.
[9] Idire S O, Asikong B E and Tiku D R 2016. Potentials of banana peel, vegetable waste (*Telfairia occidentalis*) and pig dung substrates for biogas production. *Br. J. Appl. Sci. Technol.* **16(5)** 1-6.
[10] Wang CH, Zhao D, Tsutsumi A and You S 2017. Sustainable energy technologies for energy saving and carbon emission reduction. *Appl. Energy* **194** 223-24.
[11] Ma Y, Ge Q, Li W and Xu H 2009. Methanol synthesis from sulfur-containing syngas over Pd/CeO 2 catalyst. *Appl. Catal B: Environ*. **90** 99–104.
[12] Abadi N, Gebrehiwot K, Techane A and Nerea H 2017. Links between biogas technology adoption and health status of households in rural Tigray, Northern Ethiopia. *Energy Policy* **101** 284–92.
[13] Dahunsi S O, Olayanju A, Izebere J O and Oluyori A P 2018. Data on Energy and Economic evaluation and microbial assessment of anaerobic co-digestion of fruit rind of *Telfairia occidentalis* (Fluted Pumpkin) and Poultry Manure. *Data Brief* **21** 97-104.
[14] Dahunsi S O, Oranusi S, Efeovbokhan V E, Olayanju A, Zahedi S, Ojediran J O, Izebere J O and Aladegboye O J 2018. Anaerobic conversion of *Chromolaena odorata* (Siam weed) to biogas. *Energy Reports* **4** 691–700.
[15] Dahunsi S O, Oranusi S, Efeovbokhan V E, Zahedi S, Ojediran J O, Olayanju A, Oluyori A P, Adekanye T A, Izebere J O and Enyinnaya M 2018. Biochemical conversion of fruit rind of *Telfairia occidentalis* (Fluted Pumpkin) and Poultry Manure. *Energy Sources (Part A) Utiliz. Environ. Effects* **40(23)** 2799-811.
[16] You S, Ok Y S, Chen S S, Tsang D C, Kwon E E, Lee J and Wang C H 2017. A critical review on sustainable biochar system through gasification: energy and environmental applications. *Bioresour. Technol.* **246** 242-53.
[17] Higman C and Van Der Burgt M 2003. Gasification, Gulf Professional Publishing, 2003.
[18] Xiong Q, Kong SC and Passalacqua A 2013. Development of a generalized numerical framework for simulating biomass fast pyrolysis in fluidized-bed reactors. *Chem. Eng. Sci.* **99** 305–313.
[19] Hernández J J, Aranda-Almansa G and Bula A 2010. Gasification of biomass wastes in an entrained flow gasifier: effect of the particle size and the residence time. *Fuel Process. Technol* **91** 681–692.
[20] Chopra S and Jain A 2015. A Review of Fixed Bed Gasification Systems for Biomass.
[21] Khan AA, deJong W, Jansens PJ and Spliethoff H 2009. Biomass combustion in fluidized bed boilers potential problems and remedies. *Fuel Process. Technol.* **90** 21–50.
[22] Ruiz J, Juarez M, Morales M, Munoz P and Mendívil M 2013. Biomass gasification for electricity generation: review of current technology barriers. *Renew. Sustain. Energy Rev.* **18** 174-83.
[23] Dhepe PL and Fukuoka A 2008. Cellulose conversion under heterogeneous catalysis. *ChemSusChem* **1** 969–75.
[24] Klimantos P, Koukouzas N, Katsiadakis A and Kakaras E 2009. Air-blown biomass gasification combined cycles (BGCC): system analysis and economic assessment. *Energy* **34** 708-14.
[25] Pedroso D T, Machín E B, Silveira J L and Nemoto Y 2013. Experimental study of bottom feed updraft gasifier. *Renew. Energy* **57** 311–16.
[26] Atnaw SM, Sulaiman SA and Yusup S 2013. Syngas production from downdraft gasification of oil palm fronds. *Energy* **61** 491–501.
[27] Gai C and Dong Y 2012. Experimental study on non-woody biomass gasification in a downdraft gasifier. *Intl J. Hydr. Energy* **37** 4935–44.
[28] Ong Z, Cheng Y, Maneerung T, Yao Z, Tong YW, Wang CH and Dai Y 2015. Co-gasification of woody biomass and sewage sludge in a fixed-bed downdraft gasifier. *AIChE J.* **61** 2508-21.
[29] Zhang Y, Zhao Y, Gao X, Li B and Huang J 2015. Energy and exergy analyses of syngas produced from rice husk gasification in an entrained flow reactor. *J. Clean. Prod.* **95** 273-80
[30] Food and Agriculture Organization (FAO, 1986). Gasifier Design Handbook
[31] Food and Agriculture Organization (FAO, 1960). Gasifier Design Handbook

[32] Dahunsi S O 2019. Liquefaction of pineapple peel: Pretreatment and process optimization. *Energy* **185** 1017-31.
[33] APHA, 2012. Standard Methods for the Examination of Water and Wastewater. American Public Health Association, Washington, DC, USA.
[34] Monlau F, Barakat A, Steyer JP and Carrere H 2012. Comparison of seven types of thermo-chemical pretreatment on the structural features and anaerobic digestion of sunflower stalks. *Bioresour. Technol.* **120** 241–7.
[35] Sluiter A, Hames B, Ruiz R, Scarlata C, Sluiter J and Templeton D 2008. Determination of Ash in Biomass. Laboratory Analytical Procedures (LAP). Natl. Renew Energy Lab. 1–8 Report No. TP-510-42622.
[36] Sluiter A, Hames B, Ruiz R, Scarlata C, Sluiter J, Templeton D and Crocker D 2012. Determination of Structural Carbohydrates and Lignin in Biomass. Laboratory Analytical Procedures (LAP). Natl. Renew Energy Lab. 1–18 Report No. TP-510-42618.
[37] Bazoti S F, Golunski S, Pereira S D, Scapini T, Barrilli É T, Alex M D, Barros K O, Rosa C A, Stambuk B U, Alves S L, Valério A, de Oliveira D and Treichel H 2017. Second-generation ethanol from non-detoxified sugarcane hydrolysate by a rotting wood isolated yeast strain. *Bioresour. Technol.* **244** 582–7.
[38] Patra T K and Sheth P N 2015. Biomass gasification models for downdraft gasifier: a state-of-the-art review. *Renew. Sustain. Energy Rev.* **50** 583-93.
[39] Anil M, Rupesh S, Muraleedharan C and Arun P 2016. Performance evaluation of fluidised bed biomass gasifier using CFD. *Energy Proc*. **90** 154–62.
[40] Bogdanova V, George E, Meynet N, Kara Y and Barba A 2017. Numerical CFD Simulations for Optimizing a Biomass Gasifier and Methanation Reactor Design and Operating Conditions. *Energy Proc.* **120** 278–85.
[41] Kirsanovs V, Blumberg D, Veidenbergs I, Rochas C, Vigants E and Vigants G 2017. Experimental investigation of downdraft gasifier at various conditions. *Energy Proc.* **128** 332–8.
[42] Susastriawan A A P, Saptoadi H and Purnomo S 2017. Small-scale downdraft gasifiers for biomass gasification: A review. *Renew. Sustain. Energy Rev*. **76** 989–1003.
[43] Dalmiş IS, Kayişoğlu B, Tuğ S, Aktaş T, Durgut MR and Durgut FT 2018. A Prototype Downdraft Gasifier Design with Mechanical Stirrer for Rice Straw Gasification and Comparative Performance Evaluation for Two Different Airflow Paths. *Tarim Bilimleri Dergisi–J. Agric. Sci.* **24** 329-33.
[44] Nelson L, Park S and Hubbe M A 2018. Thermal depolymerization of biomass with emphasis on gasifier design and best method for catalytic hot gas conditioning. *BioResour.* **13(2)** 4630-727.
[45] Xiong Q, Yeganeh MM, Yaghoubi E, Asadi A, Doranehgard MH and Hong K 2018. Parametric investigation on biomass gasification in a fluidized bed gasifier and conceptual design of gasifier. *Chem. Eng. Proc: Proc. Intens.* **127** 271–91.
[46] Yan W, Shen Y, You S, Sim SH, Luo Z, Tong YW and Wang C 2018. Model-based downdraft biomass gasifier operation and design for synthetic gas production. *J. Clean. Prod.* **178** 476-93.
[47] Dairo O U, Olayanju T M, Ajisegiri E S and Alamu O J 2013. Optimization of in-situ biodiesel production from raw castor bean seed. *J. Eng. Technol. Policy* **3(13)** 14-19.
[48] Dairo OU, Olayanju TMA, Amusan O, Adeosun OJ and Adeleke AE 2013. Production of biodiesel from *Jatropha curcus* seed using in situ techniques (Effects of catalyst amount and alcohol-seed ratio). *LAUTECH J. Eng. Technol.* **7(1)** 37-43.